Combining multiple sub-1 GHz frequencies in Radio Tomographic Imaging

Reference:

Denis Stijn, Berkvens Rafael, Ergeerts Glenn.- Combining multiple sub-1 GHz frequencies in Radio Tomographic Imaging 2016 International Conference on Indoor Positioning and In door Navigation (IPIN), 4-7 October, 2016, Madrid, Spain - ISSN 2471-917X - IEEE, 2016, p. 1-8

Full text (Publishers DOI): http://dx.doi.org/doi:10.1109/IPIN.2016.7743620

2016 International Conference on Indoor Positioning and Indoor Navigation (IPIN), 4-7 October 2016, Alcalá de Henares, Spain

Combining Multiple Sub-1 GHz Frequencies in Radio Tomographic Imaging

Stijn Denis, Rafael Berkvens, Glenn Ergeerts, Ben Bellekens, and Maarten Weyn
MOSAIC, Faculty of Applied Engineering
University of Antwerp – iMinds
Antwerp, Belgium
stijn.denis@uantwerpen.be

***Abstract*—Conventional localization systems require the target to carry a tag, which can be highly impractical for some individuals, such as the elderly, or in some situations, such as in emergencies. This requirement can be alleviated by an emerging set of tagless or device-free localization systems, of which Radio Tomographic Imaging (RTI) is a common example. Most variations of this technique assume the use of radio frequency (RF) signals in the 2.4 GHz band, or combinations of lower frequencies with that band; however, using only lower frequencies might decrease the power consumption and the influence of the environment, and increase the range of the system. We tested the combination of 433 MHz and 868 MHz in a single RTI system. We studied two approaches to combine the RTI images generated by one frequency with the other: an approach based on literature and a newly developed approach based on probability theory. This paper compares the result of both approaches. We found that the result based on literature has a root-mean-square error (RMSE) of 1.09 m, while our approach has an RMSE of 0.54 m. While also improving the state-of-the-art fusion of two frequencies, we proved the feasibility of combining only frequencies under 1 GHz in an RTI system.**

***Index Terms*—radio tomographic imaging, device-free localization, sub-1 GHz frequencies, tagless localization**

I. Introduction

Over the years, many different technologies for accurately locating individuals or objects have been developed. Common examples of such technologies are GPS, Wi-Fi, and active infrared [1]–[3]. Most of the systems applying these technologies require their targets, the entities which are to be located, to each carry an active hardware device, a 'tag'. Presently, adaptive localization algorithms largely eliminate the need for these tags to be specialized, dedicated hardware [4]. Nevertheless, depending on the application, the requirement to carry a tag can be highly impractical (*e.g.*, people in danger who need to be located quickly by emergency services) and might cause the system to suffer from a lack of consumer acceptance. For this reason, there has been a growing interest in localization systems where the use of a tag is unnecessary: tagless or device-free localization. These localization techniques rely on the influence which the presence of the entities themselves has on its environment.

Device-free localization within a clearly defined environment is comprised of three different aspects: detection, tracking and identification [5]. Detection refers to the ability of the system to determine whether or not there are changes in the environment and if so, how many separate entities are causing these changes. Tracking refers to the tracking of the positions of entities within the environment. The current possible locations of entities causing changes are determined. An entity is tracked (a velocity and a sequence of positions of an entity over a duration of time are estimated) based on a series of location estimations (estimations of the location of an entity at one time). Tracking can be performed for a single entity or for multiple entities simultaneously (multi-tracking). Finally, identification can be understood as determining the identity of the detected and tracked entities. The term 'identity' is loosely defined in this context and can refer to the size, shape, type of the entity or to an actual identity of an individual. This is one of the most difficult problems in device-free localization and there has been very little research regarding this domain.

One highly interesting approach to tagless localization utilizes the changes caused by an individual on a radio frequency (RF) signal to infer their position. A big advantage of RF-based localization techniques lies in the fact that RF signals can easily pass through (non-metallic) walls. Companies like Time Domain [6] and Camero Tech [7] have developed UWB-based TTW-imaging products which transmit UWB-signals and then measure echoes to estimate a range and bearing. However, constructing a tagless localization system using these highly complex products can be rather expensive. Additionally, they tend to have noise and accuracy related problems at long range [8]. Using a multitude of cheap low-capability collaborating nodes which measure transmission rather than scattering and reflection is a far more cost efficient solution. These nodes are all capable of transmitting and/or receiving wireless signals, thereby creating an entire network of links that pass through the environment. Such a network is called an RF sensor network. Due to multipath effects, a moving object or individual standing in the Line-of-Sight (LoS) of a link between two nodes will cause the characteristics of the link to change. Based on the nature of these changes, the moving entity can be located and tracked. Because each link between two RF sensors measures a section of the environment space, techniques based on this principle are called tomographic techniques.

One such technique based on the use of a tomographic

RF sensor network consists of estimating an image of the changes in environment based on the Received Signal Strength (RSS) of each link. This is called Radio Tomographic Imaging (RTI) [9]. Several different variations of RTI exist, ranging from basic localization techniques based on expected shadowing loss [10] to fully-fledged systems incorporating advanced multi-tracking algorithms [11] and multi-channel approaches [12].

In nearly all existing RTI systems, the 2.4 GHz frequency band is used [10]–[12]. It is only recently that interest has been shown in the use of other frequencies. An adaptation of the original RTI algorithm for the 800/900 MHz band is made in [13]. In [14], 868 MHz and 2.4 GHz are combined in a single RTI system. A 433 MHz RTI system is combined with a tagged RSS based trilateration localization method in [15].

We constructed and implemented a multi-frequency RTI system using 433 MHz and 868 MHz in an open indoor environment of 60 m^2. RTI images are created when an individual is present in the environment. This is done separately for each frequency. Next, we combine the two images in two ways: one based on literature [14], and a new approach based on probability theory. We compare the positioning results of the two techniques.

The remainder of this paper is organized as follows. The basic concept of RTI and several RTI variations are described in Section 2. Section 3 contains the methodology used in the construction of the RTI system and the analysis of the resulting images. Section 4 shows and discusses the results of our experiments with the multi-frequency system. In Section 5, we show possible interesting future research directions regarding RTI and present a conclusion for the research in this paper.

II. Radio Tomographic Imaging

Radio Tomographic Imaging (RTI) is a tagless localization technique which estimates an image representing changes occurring in an environment. These estimations are based on the RSS values of each link in a tomographic RF sensor network. The basic principle of an RTI measurement model is as follows [8]–[10]:

First, an environment containing an RF sensor network is defined. This environment is divided into N number of pixels. Next, a vector $\boldsymbol{y}$ of size M is defined, containing all RSS measurements for every link in the RF sensor network. Another vector $\boldsymbol{x}$ is also defined, containing the likelihood of whether a moving object is present, for every pixel. During the following step, a weighting matrix W of dimension M x N is defined with each column representing a single pixel and each row describing the weighting of each pixel for that link. With n representing noise, vector $\boldsymbol{y}$ can then be described as:

$$\mathbf{y} = W\mathbf{x} + n \tag{1}$$

The goal of RTI is to approximate this vector $\boldsymbol{x}$, which represents the desired attenuation image. Pixels in which strong attenuation is present are likely to contain individuals. There are many different ways to accomplish this. In the next sections, several important aspects and different types of RTI models will be discussed.

A. Regularization

Trying to solve the equation in the previous paragraph for vector $\boldsymbol{x}$ is an ill-posed inverse problem. A single, unique solution does not exist. If we approximate $\boldsymbol{x}$ by calculating the least squares solution, the noise n is amplified to such a degree that the result becomes essentially meaningless. Therefore, *regularization* (introducing additional information to the model in order to stabilize the problem) is necessary. Possible regularization methods for RTI are discussed in [16]. The chosen regularization method has a large impact on the smoothness of the resulting tomographic image.

B. Shadowing-based RTI

A basic, linear RTI model is presented in [9] and [10]. It is also called shadowing-based RTI [8]. Vector $\boldsymbol{y}$ contains a list of differences between the averaging of several initial calibration measurements (performed when no moving entities were present in the environment) and live measurements taken when the system is active. A Maximum A Posteriori (MAP) formulation is used when trying to determine $\boldsymbol{x}$. This leads to the following formula:

$$x_{MAP} = (W^T W + C_x^{-1}\sigma^2_{Noise})^{-1} W^T y \tag{2}$$

where W is an M x N (with M: total number of links, N: total number of pixels) weighting matrix which describes the attenuation impact of every pixel for every link. The value of each element of W is given by $W_{ij} = 1/\sqrt{d_i}$ (with d_i = distance between the nodes comprising link i, expressed in number of pixels) provided that the pixel lies within an ellipse with foci at the node locations for that link. The width of this ellipse is described by a constant parameter λ. It is strongly influenced by the size of the first few Fresnel zones of the links. C_x is an *a priori* N x N (N: number of pixels) covariance matrix, based on the initial assumption that $\boldsymbol{x}$ is a zero-mean Gaussian random field. It is created using an exponential spatial decay:

$$[C_x]_{kl} = \sigma_x^2 * e^{-d_{kl}/\delta_c} \tag{3}$$

where d_{kl} is the distance between pixels k and l, δ_c is a space constant which determines the smoothness of the resulting image and σ_x^2 is the variance at each pixel. This matrix is responsible for regularization. The vector $\boldsymbol{y}$ contains all of the differences between the current link strengths and previous calibration measurements. The desired attenuation image vector is x_{MAP}, the value of each element of this vector being expressed in dB. Finally, σ^2_{Noise} represent noise-variance. Usually, the noise is Gaussian.

Experimental results indicate accurate localization of two separate moving entities. These experiments took place in a 4.27 m by 4.27 m, mostly empty environment. It is represented by 25 x 25 pixels using an RF sensor network of 28 nodes [9].

In our experiments, we only use simple shadowing-based RTI. The focus of this project lies in the research of the

changing characteristics of RF links of different frequencies when a human target is present, not in the simulation of an advanced RTI system.

C. Variance-based RTI

One important disadvantage of shadowing-based RTI lies in its assumption that a moving entity blocking the LoS path of a link will simply cause a decrease of the RSS value for that link. Due to multipath effects, this is not always the case, especially for links that cross one or multiple indoor walls. As a result of this faulty assumption, accurate shadowing-based through-wall imaging in cluttered environments is almost impossible.

Instead of considering $\boldsymbol{y}$ to be a vector consisting of differences between calibration measurements and current measurements, Variance-based RTI (VRTI) uses the windowed variance of each link's RSS values [17]. An additional advantage of this approach lies in the fact that initial calibration measurements are no longer necessary. This makes VRTI well suited for emergency applications like hostage situations or building fires where the police or emergency workers quickly need to be aware of moving entities in an unknown environment.

When this technique is combined with a Kalman filter, experimental results show an error margin between 1 and 2 meter when tracking a single individual. These results are acquired within a building that is part of an environment of size 9.1 m by 9.1 m [17].

D. Channel Diversity

A possible way to improve the accuracy of RTI systems, is to make use of different channels within the RF sensor network which the RTI system utilizes. It is important to note that this differs from the use of multiple frequency bands, as each channel still lies within the same band. In [12], a technique is proposed in which multiple channels in an RTI system are sorted based on fade level. Links in a deep fade are not considered to be reliable indicators of the presence of an entity in the LoS of the link. Anti-fade links are much more desirable. By utilizing multiple channels at the same time, more links in general and consequently more links in anti-fade are created, which improves the accuracy of the system. Interestingly, through-wall motion tracking with a simple attenuation based RTI system in a cluttered environment becomes possible once multiple channels are used [12].

E. Multiple Frequencies

As stated earlier, the vast majority of Radio Tomographic Imaging systems only utilize the 2.4 GHz frequency band. One of the first adaptations of RTI for use in other bands was made in [13]. In their research, they describe the potential advantages of the use of sub-1 GHz frequencies and construct an 868 MHz RTI system. This system achieved a maximum average localisation error below 78 cm in a 5 m x 5 m open indoor environment. In [14], an RTI system is demonstrated which combines 2.4 GHz and 868 MHz in a complex office environment. When comparing the estimated positions to the actual positions, an RMSE of 26 cm was obtained. A combination of a tagged RSS based trilateration localization method and a 433 MHz RTI system is described in [15]. A positioning error below 1 m was obtained in 90% of all cases in a 4 m x 4 m indoor environment. A major advantage of using sub-1 GHz frequencies in RTI are the possibility of constructing a more energy-efficient design. Additionally, the effects of reflections and multi-path propagation are lessened, which can lead to a more accurate localization in some complex environments. This can clearly be seen in [14], where a single-frequency 868 MHz configuration obtained more accurate results than the 2.4 GHz configuration due to the complexity of the environment. Furthermore, the use of lower frequencies can lead to a larger range and therefore increases the size of the environments in which an RTI system can be deployed. An important downside, however, is the fact that the attenuation caused by human presence in the environment is considerably lower. Depending on the complexity of the environment, this can negatively impact the accuracy rather strongly. In regular environments, a 2.4 GHz implementation will nearly always be more accurate.

III. Methodology

A. Initial Experiment

The very first step of our research consists of empirically verifying the suitability of 433 and 868 MHz for use in RTI with a simple experiment. In this experiment, we investigate the impact that the presence of an individual has on a single link for both 433 and 868 MHz.

We construct our setup in the middle of an empty outdoor football field. Two Silicon Labs WSTK6200 development board paired with an EZR32 Leopard Gecko radio board [18] are set up at a height of 1 m at a distance of 7 m from each other. They are both equipped with a sub-1 GHz antenna and used to represent nodes in a real RTI system. The modules communicate with each other using the DASH7 Alliance Protocol (D7AP), a low power open wireless sensor and actuator network standard which can communicate on the 433, 868, and 915 MHz bands [19].

One of the two nodes is connected to a computer with an FTDI-cable. When a button is pressed on this node, it sends a packet to the other node. The other node receives the packet and sends a response containing the RSS value with which it was received. The first node receives and sends both the RSS value inside the packet as the RSS value with which it received the packet to the computer. The average of these two values is calculated in order to obtain an RSS value for the link. This entire process is then automatically repeated for the other frequency band.

We measured the RSS value once a person was present in the LoS and close to it. The person stood at six different locations within the LoS and at one, two, and three meters distance from it. We also measured the RSS values when no one was present as calibration measurements. The difference between the measurements with a person and the calibration measurements are shown in Figure 1. The dotted lines represent the first five Fresnel zones. It is important to note that

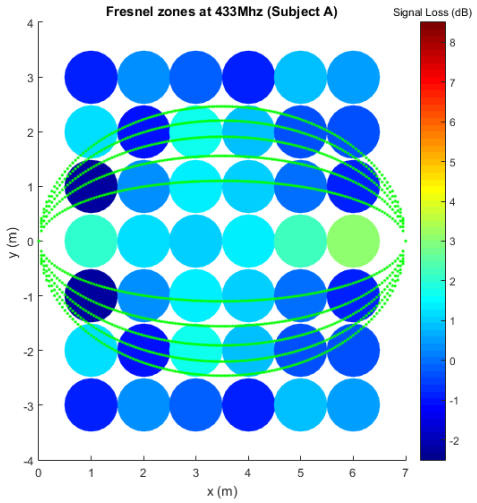

(a) 433 MHz

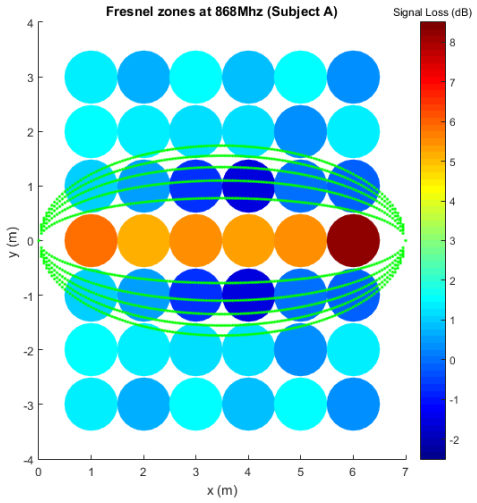

(b) 868 MHz

Fig. 1. Attenuation of the 433 MHz and 868 MHz communication links when an individual is located within the environment. The color of each circle indicates the link attenuation when an individual is present in that location. A negative attenuation indicates amplification. Data is mirrored on one side.

measurements were taken for human presence on only one side of the link. Theoretically, this should not matter in an ideal environment, therefore the data in this figure is mirrored on one side for clarity. For 868 MHz, there is a large amount of attenuation when an individual is standing in the line-of-sight. The impact the subject has on the RSSI value of the link also clearly reduces as they move further away from the link. However, due to the fact that this human presence often overlaps multiple Fresnel zones, it is not possible to simply determine for any given position whether human presence will cause the power to increase or decrease based on whether they are standing in an odd or even numbered Fresnel zone [20]. Nevertheless, the use of 868 MHz in RTI is clearly possible.

For 433 MHz, the attenuation is considerably smaller in the line-of-sight. Human presence can also influence the link value

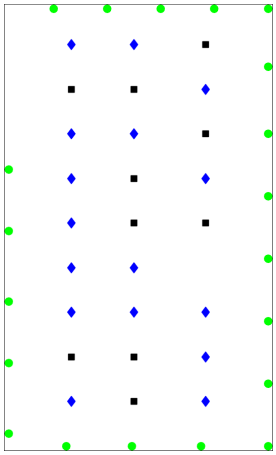

Fig. 2. Schematic overview of the environment. Green circles indicate node locations, blue diamonds indicate training locations and black squares indicate test locations.

from farther away, increasing the total amount of noise, from the point of view of an RTI system. This matches theoretical predictions, due the fact that the larger wavelength leads to larger Fresnel zones. Still, we consider the LoS attenuation to be sufficient for use of the frequency band in RTI. It does, however, either need to be used in combination with another system or frequency and/or be utilized in an environment with a very large link density. This is indeed the case in [15].

B. Construction of a Multi-Frequency Tomographic Sensor Network

All available nodes are used in the multi-frequency tomographic network we construct. It consists of 20 transceiver nodes. Just as in the experiment mentioned in the previous section, each node communicates using the DASH7-standard and consists of a Silicon Labs WSTK6200 development board paired with an EZR32 Leopard Gecko radio board. A schematic of the network as it will be installed in the environment is presented in Figure 2.

Essentially, the communication schedule which is used in the network is partially based on the timed-token passing protocol described in [21] and [14] with some added features in order to improve the flexibility of the system and incorporate the possibility of switching between frequencies on a single piece of hardware. Functionally speaking, there are two types of nodes: one sub-controller and a set of regular nodes. The sub-controller regulates the network and passes on the RSS data to the computer on which the RTI algorithm will be run. A node only has to broadcast a so-called RTI message to the entire network once it receives a message from the previous node.

The steps for setting up the network are described in the following paragraphs.

First, a sub-controller is placed in the environment and connected to a computer. On start-up, the sub-controller is in configuration mode. It is ready to receive all requests from nodes to join the RTI network.

Second, the regular RTI nodes are placed in the environment and powered. They can then be instructed with a button press to broadcast a 'Join Network' packet to a potential sub-controller within range. All communication related to the configuration of the network is performed in the 433 MHz frequency band.

Third, if the sub-controller receives a 'Join Network' packet, it increases an internal network size counter by one and responds to the node with a 'Join Network Response' containing a node number. This number determines the order in which the nodes will sent during a scan cycle. The sub-controller is considered to have node number 0.

The sub-controller can now be instructed to begin the scan cycles by way of a button press. It switches to RTI mode and broadcasts its first RTI message packet on the 433 MHz frequency band. Once the sub-controller is in RTI mode, the communication schedule is as follows.

First, the RTI packet is received by all nodes in the network. Each node saves the RSS value with which it received the message in an RSS list. Every node updates its RSS list for each RTI message it receives. It contains the RSS values of the last message that was received from all other nodes in the network. If an RTI message is received from a new node for the first time, the size of the list increases.

Second, because the packet that was received by node 1 was sent by node 0 (the sub-controller), it is now node 1's turn to broadcast an RTI packet. Once node 2 receives this packet, it knows that it is his turn to send, and so on. The maximum time between node 1 and node 2 sending is 25 ms. The RTI packets send by the regular nodes contain the entire RSS list of that node. When the sub-controller receives these packets, it does not only merely update its own RSS list like the regular nodes, but also saves this data in an RSS matrix. This matrix contains all RSS data from every node in the network.

Third, once the final node in the network has sent an RTI packet, the sub-controller updates the RSS matrix once more. Afterwards, it sends this RSS matrix over the UART to the computer it is connected to. In a real-time RTI system, this data is directly used as input to an RTI algorithm that is running on this computer. In our experiments, the data is saved to a file which is analyzed at a later time.

Fourth, the sub-controller broadcasts a 'Band Switch' message. The nodes receive this message and switch to 868 MHz. The cycle then begins again. The nodes and the sub-controller use separate lists and matrices for each frequency band.

Finally, with another button press, the sub-controller can go back to configuration mode. If the sub-controller receives RTI messages while in this mode (which occurs because the button will most likely be pressed in the middle of a scan cycle), it saves the data in the RSS matrix as usual. Once the last node in the network has sent its packet, the sub-controller sends out one final RTI message containing a special value informing all of the nodes that this is the last cycle. After the last node has broadcast its RTI packet, all communication ceases and new nodes can once again be added to the network.

It is sometimes possible that a packet is not received by a network node. Systems are in place to deal with the following two cases:

1) If a regular node fails to receive an RTI message from the previous node, the network grinds to a halt. Every node will be waiting for a message from its previous node, but no new packets will be sent. After a certain amount of time t has passed, the sub-controller will notice that it has not received any RTI messages. It will then decide to skip this scan cycle entirely, sent a 'Band Switch' packet and start anew.
2) If a regular node fails to receive an RTI message from a node that is not the previous node in between the time of the node sending during scan cycle i and sending during scan cycle $i + 1$, it changes the value for that node in its RSS list to 0. In doing so, the responsibility for handling these cases is passed to the RTI algorithm running on the computer.

It is important to note that all of the data in a single RSS matrix is not collected at the exact same time. During scan cycle i, node 1 will transmit a list with RSS values which have mostly been collected during scan cycle $i - 1$ (for that frequency). The sole exception is the value pertaining to node 0, which was collected during the most recent cycle. For node 2 the same principle applies, with the values for all nodes except for node 0 and node 1 having been collected during the previous scan cycle. This could lead to a possible slight increase in position estimation error.

C. RTI algorithm

When analyzing an RSS matrix, the first step always consists of averaging the two corresponding RSS values of two nodes comprising a single link and doing so for each link. This results in a vector containing the RSS value of all links. If one of the 2 RSS values is equal to zero, meaning that there was no two-way communication during this scan cycle, the other value is used. If both values are equal to zero, no communication has taken place between those two nodes, leading to one less link in the environment. As this occurs only very sporadically in our setup, RSS matrices containing one or more missing links are discarded. As stated earlier, in this paper we implement a basic shadowing-based RTI system.

Multiple measurements are performed in an empty environment, which are then averaged to be used as calibration data. The differences for each link between live measurements and the calibration data are collected in a vector $\boldsymbol{y}$ which is then plugged into the formula given in (2). This results in the creation of an image vector which represents the attenuation occurring in each pixel. All of these steps are performed separately for 433 MHz and 868 MHz data, leading to two different images.

D. Combining RTI images

The main goal of this research is to investigate the possibilities of combining two sub-1 GHz frequencies in a single RTI system. Therefore, we must find a way to combine the

information obtained from both 433 and 868 MHz. In [14], a method is proposed in which the results for 2.4 GHz and 868 MHz are simply added. This methodology assumes, however, that the attenuation influence of an obstacle follows the same pattern regardless of frequency. Due to the differently sized Fresnel zones, this is clearly not the case. We propose a second method which transforms an image vector into a probability vector, with each element representing the probability that someone is present in the corresponding location. We then calculate the point-wise product of these vectors in order to obtain a combined vector.

By applying Bayes' theorem, we can express the probability of an entity being present for each pixel as:

$$P(A_i \mid x_i) = \frac{P(x_i \mid A_i)P(A_i)}{P(x_i \mid \overline{A_i})P(\overline{A_i}) + P(x_i \mid A_i)P(A_i)} \quad (4)$$

where $P(A_i \mid x_i)$ represents the probability of an entity being present at pixel x_i. $P(x_i \mid A_i)$ is the likelihood of the value x_i given that someone is present. $P(A_i)$ represents the *a priori* probability that an individual is present at a certain pixel, regardless of x_{MAP} values.

In order to determine the value of $P(x_i \mid A_i)$ and $P(x_i \mid \overline{A_i})$, extra training steps besides the initial calibration are necessary. We perform measurements for when an individual is present in a number of training locations in our environment and apply all the regular steps of shadowing-based RTI until we obtain a series of RTI images. Next, we take the values of all pixels in these RTI images which lie within a certain radius r of the true locations of the individuals and calculate a normal distribution. The probability density function of this distribution represents $P(x_i \mid A_i)$. Similarly, a normal distribution is fitted to the values of all pixels which lie outside a radius r of the true locations. This leads to $P(x_i \mid \overline{A_i})$.

$P(A_i)$ is determined empirically. An interesting future research topic would be to investigate the possibility of a live RTI system dynamically changing this parameter based on how often it detected the presence of one or more individuals. This lies beyond the scope of this paper, however.

Both the additive method as well as the method based on probability will be performed and the results will be compared.

E. Positioning

Once we have obtained an RTI image which combines the results from both frequencies, we can move on to the final step: determining the number and estimating the locations of individuals present in the environment. A weighted centroid-based approach is used in combination with a threshold. This approach is based slightly on the positioning procedure with proximity scans proposed in [22].

First, a threshold is applied to the entire RTI image. This threshold is calculated according to the following formula:

$$T = \lambda * max(x) \quad (5)$$

With x being the whole RTI image and λ an empirically determined parameter. Next, the weighted centroids are calculated of the still remaining connected components whose size is equal to or larger than a second threshold t. This threshold is also determined empirically. The coordinates of these centroids are considered by the system to be the location of individuals present in the environment.

Fig. 3. Photograph of the environment

IV. Results

We construct the tomographic sensor network described in Section 3 in an open indoor classroom environment of size 10 m x 6 m. All 20 nodes are distributed along the edge of the environment wherever feasible. Additionally, we select 26 locations where an individual will be present. We want to use approximately 60% of these positions as training data for our probabilistic model. As a result, 16 locations are randomly selected to be used for this purpose. The accuracy of our localization system will be assessed by using the remaining 10 locations as test data. All of these locations are indicated in Figure 2. A photograph of the environment is presented in Figure 3. First, we generate RTI images for all of our test locations and both of our frequencies. In Figure 4, two 433 MHz image vectors and two 868 MHz image vectors are shown. By themselves, the 433 MHz RTI images do not appear to be appropriate for use in localization. Attenuations near the actual locations are fairly low and many local maximums are far removed from the correct positions. 868 MHz fares somewhat better, as in (b) the largest attenuations are clustered around the correct location. However, the image vector in (d) appears to suffer from the same problems as the 433 MHz images. From a purely visual point of view, we can already see the benefits that combining these images would bring. The local maximums in (c) and (d) are spread out throughout the images, but match for both frequencies at the correct location.

In our next step, we combine the RTI images. As stated earlier, we do so for two different methods: an addition-based method and a probabilistic method. Figure 5 shows the combined RTI images for the same locations as those presented in Figure 4.

The probabilistic approach looks to be quite successful, as the remaining clusters all encapsulate or are very close to the actual location. For the addition-based method quite a few clusters still remain, although in both (a) and (b) the clusters containing the pixels with the largest attenuation are also very close to the correct positions.

Our final step consists of applying our weighted centroid-based positioning method in order to obtain an actual location. Results are shown in Figure 6. In all cases, the estimated

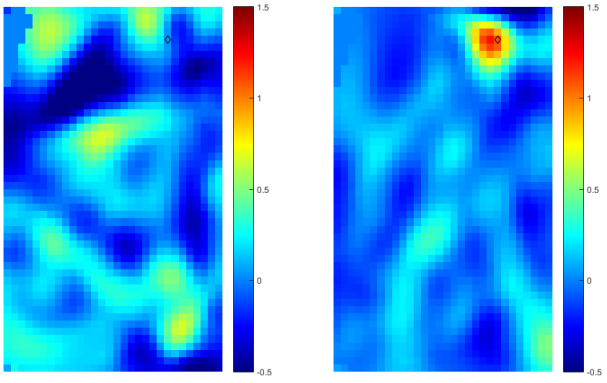

(a) RTI - 433 MHz (b) RTI - 868 MHz

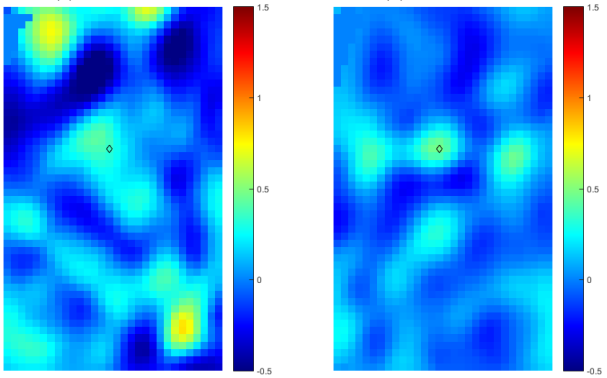

(c) RTI - 433 MHz (d) RTI - 868 MHz

Fig. 4. RTI images for 433 and 868 MHz. Actual locations are indicated by the black diamond. Pixel values in dB.

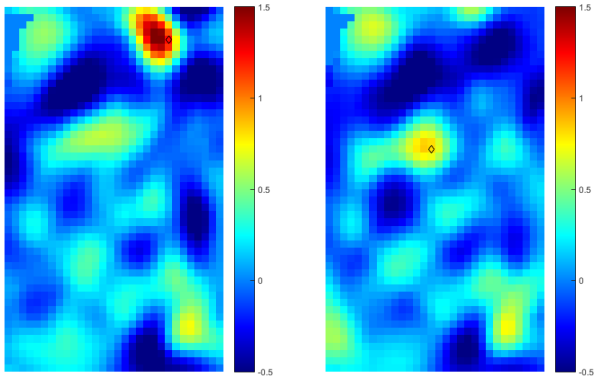

(a) RTI - Combined - Addition-based method (b) RTI - Combined - Addition-based method

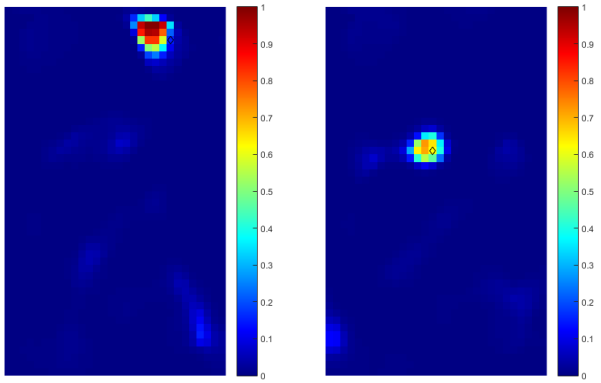

(c) RTI - Combined - Probabilistic method (d) RTI - Combined - Probabilistic method

Fig. 5. Combined RTI images. Actual locations are indicated by the black diamond. Pixel values for non-probabilistic images in dB.

TABLE I
ERROR STATISTICS FOR POSITION ESTIMATION USING 33 DATA SETS

	RMSE [m]	false negatives	false positives
868 MHz	2.325	0	9
433/868 MHz Addition	1.093	0	6
433/868 MHz Probabilistic	0.544	1	0

position appears to be remarkably close to the actual location. In (b), we can see that two clusters exist after image-wide thresholding was applied, but due to the small size of one of the clusters, this was correctly ignored.

We perform the aforementioned steps in all 11 locations with data that was collected during 3 different scan cycles. This means that this localization technique is evaluated based on 33 data sets. We compare a single-frequency 868 MHz approach, a multi-frequency approach based on the addition method and a multi-frequency approach based on our probabilistic model. Error statistics are presented in table I.

All experiments are performed for one individual present in the environment. If the positioning system faultily detects an empty environment, it is counted as a false negative. If more than one individual is detected, it is considered to be a false positive. The RMSE is calculated for those cases in which the amount of individuals present is estimated correctly.

It appears that the use of the probabilistic method clearly leads to the lowest RMSE and number of false positives, although it is slightly more vulnerable to false negatives. This is due to the fact that our probabilistic approach essentially consists of a multiplication of probabilities. If one of the two probability vectors assigns a very low probability to the actual location, a possibly good result from the other vector is utterly negated. Fortunately, this appears to occur only rarely.

The most important problem with the addition-based (and the single-frequency) method is the large amount of false positives. In the previously shown RTI figures, it was already made clear that correct thresholding was necessary to eliminate the large amounts of clusters that still remained. The same problem leads to the larger RMSE-values when compared to the probabilistic method, as in some cases the clusters around the actual location are filtered away, while nearby clusters remain.

V. CONCLUSION & FUTURE WORK

We have successfully managed to construct a fully fledged multi-frequency RTI system which combines two sub-1 GHz frequency bands. The system is accurate, with an RMS positioning error of 0.54 m compared to 1.09 m of a state-of-the-art method, when implemented in an open indoor environment of size 10 m x 6 m. These results confirm that an accurate RTI

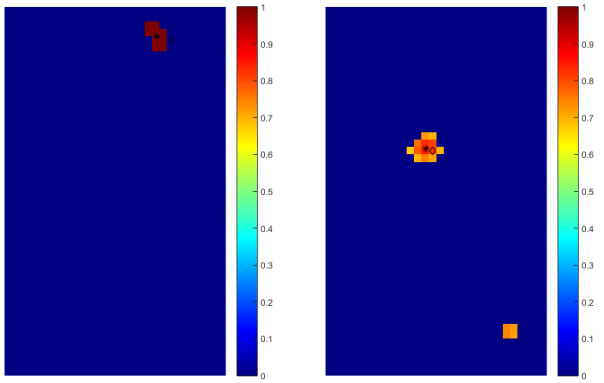

(a) RTI - Combined - Addition-based method

(b) RTI - Combined - Addition-based method

(c) RTI - Combined - Probabilistic method

(d) RTI - Combined - Probabilistic method

Fig. 6. Combined RTI images after positioning. Actual locations are indicated by the black diamond. Pixel values for non-probabilistic images in dB.

system which utilizes only sub-1 GHz frequencies is possible. While the use of 433 MHz in a single frequency system is very difficult unless a large amount of nodes is used, here it was successfully used in combination with 868 MHz. Our best results were obtained by combining the separate RTI images for each frequency using a probabilistic model, which significantly outperformed an addition based approach. The probabilistic model was slightly more susceptible to false negatives, however. This is a problem that will likely worsen when the system is implemented in more complex environments, and certainly bears looking into for future research.

One of the main advantages of the use of sub-1 GHz frequencies is the increased range. Currently, we are looking into the feasibility of a sub-1 GHz RTI system in a large scale, outdoor environment. The primary focus here will lie on using RTI principles to estimate the amount of individuals present in the environment, not on outright localization. The knowledge gained in these experiments will eventually be used to improve multi-tracking with RTI in general and to quantify the relationship between environment size, system accuracy and the amount of RTI nodes that are present.

Acknowledgement

Part of this work has been funded by the iFest project, cofunded by iMinds and VLAIO.

References

[1] J. Paek, J. Kim, and R. Govindan, "Energy-efficient rate-adaptive gps-based positioning for smartphones," in *Proceedings of the 8th international conference on Mobile systems, applications, and services*. ACM, 2010, pp. 299–314.

[2] E. C. Chan, G. Baciu, and S. Mak, "Using wi-fi signal strength to localize in wireless sensor networks," in *Communications and Mobile Computing, 2009. CMC'09. WRI International Conference on*, vol. 1. IEEE, 2009, pp. 538–542.

[3] N. Bulusu, J. Heidemann, and D. Estrin, "Gps-less low-cost outdoor localization for very small devices," *Personal Communications, IEEE*, vol. 7, no. 5, pp. 28–34, 2000.

[4] M. Weyn, "Opportunistic seamless localization," *PhD, Universiteit Antwerpen*, pp. 58–64, 2011.

[5] M. Youssef, M. Mah, and A. Agrawala, "Challenges: device-free passive localization for wireless environments," in *Proceedings of the 13th annual ACM international conference on Mobile computing and networking*. ACM, 2007, pp. 222–229.

[6] "Time Domain Corporation," "http://www.timedomain.com/", Page retrieved on 11/07/2016.

[7] "Camero Tech," "http://www.camero-tech.com/", Page retrieved on 11/07/2016.

[8] A. J. Wilson, "Device-free localization with received signal strength measurements in wireless networks," Ph.D. dissertation, The University of Utah, 2010.

[9] J. Wilson and N. Patwari, "Radio tomographic imaging with wireless networks," University of Utah, Tech. Rep.

[10] ——, "Radio tomographic imaging with wireless networks," *Mobile Computing, IEEE Transactions on*, vol. 9, no. 5, pp. 621–632, 2010.

[11] M. Bocca, O. Kaltiokallio, N. Patwari, and S. Venkatasubramanian, "Multiple target tracking with rf sensor networks," *Mobile Computing, IEEE Transactions on*, vol. 13, no. 8, pp. 1787–1800, 2014.

[12] O. Kaltiokallio, M. Bocca, and N. Patwari, "Enhancing the accuracy of radio tomographic imaging using channel diversity," in *Mobile Adhoc and Sensor Systems (MASS), 2012 IEEE 9th International Conference on*. IEEE, 2012, pp. 254–262.

[13] S. Adler, S. Schmitt, and M. Kyas, "Device-free indoor localisation using radio tomography imaging in 800/900 mhz band," in *Indoor Positioning and Indoor Navigation (IPIN), 2014 International Conference on*. IEEE, 2014, pp. 544–553.

[14] A. Fink, T. Ritt, and H. Beikirch, "Redundant radio tomographic imaging for privacy-aware indoor user localization," in *Indoor Positioning and Indoor Navigation (IPIN), 2015 International Conference on*. IEEE, 2015, pp. 1–7.

[15] A. Jimenez and F. Seco, "Combining rss-based trilateration methods with radio-tomographic imaging: Exploring the capabilities of long-range rfid systems," in *Indoor Positioning and Indoor Navigation (IPIN), 2015 International Conference on*. IEEE, 2015, pp. 1–10.

[16] J. Wilson, N. Patwari, and F. G. Vasquez, "Regularization methods for radio tomographic imaging," in *2009 Virginia Tech Symposium on Wireless Personal Communications*. Citeseer, 2009.

[17] J. Wilson and N. Patwari, "See-through walls: Motion tracking using variance-based radio tomography networks," *Mobile Computing, IEEE Transactions on*, vol. 10, no. 5, pp. 612–621, 2011.

[18] *User Manual EZR32LG 868MHz Wireless Starter Kit*, 1st ed., Silicon Labs.

[19] M. Weyn, G. Ergeerts, R. Berkvens, B. Wojciechowski, and Y. Tabakov, "Dash7 alliance protocol 1.0: Low-power, mid-range sensor and actuator communication," in *Standards for Communications and Networking (CSCN), 2015 IEEE Conference on*. IEEE, 2015, pp. 54–59.

[20] P. Modes, "Basics of radio wave propagation," 2006.

[21] S. Savazzi, M. Nicoli, and M. Riva, "Radio imaging by cooperative wireless network: Localization algorithms and experiments," in *Wireless Communications and Networking Conference (WCNC), 2012 IEEE*. IEEE, 2012, pp. 2357–2361.

[22] B. Wagner, T. Ritt, and D. Timmermann, "Multiple user recognition with passive rfid tomography," in *Positioning, Navigation and Communication (WPNC), 2014 11th Workshop on*. IEEE, 2014, pp. 1–6.